Precipitation and Environmental Conditions during Accretion in Canadian East Coast Winter Storms

R. E. STEWART,* R. W. CRAWFORD,* N. R. DONALDSON,* T. B. LOW** AND B. E. SHEPPARD*

*Atmospheric Environment Service, Downsview, Ontario
**KelResearch Corporation, Downsview, Ontario

(Manuscript received 11 May 1989, in final form 10 November 1989)

ABSTRACT

Precipitation and environmental conditions occurring during accretion in Canadian east coast winter storms are described and investigated. Accretion is generally associated with snow, freezing rain, and ice pellets within saturated conditions. Precipitation types are sometimes invariant but usually evolve during individual accretion events. Accretion events are also generally associated with moderate wind speeds (average of 7.5 m s^{-1}) and warm temperatures (between $-1°$ and 0°C are most common). Remote sensing of particle shapes and terminal velocities are capable of identifying some of the features of these precipitation types. Model calculations indicate that a detailed understanding of precipitation characteristics, such as the nature of wet snow, is needed to accurately simulate accretion.

1. Introduction

Ice and snow accretion cause a large amount of damage in winter storms with consequences ranging from slight to disastrous. To better understand the conditions producing accretion and to eventually better predict these situations, detailed studies of accretion events must be made.

Two complementary problems need to be examined. One is to understand the process through which ice is affixed to structures, and the other, to understand the meteorological conditions that lead to accretion.

A great deal of attention has been devoted to modeling accretion processes (see for example, Lozowski et al. 1983; Makkonen 1984). Most laboratory experiments and field studies have concentrated on accretion due to single types of precipitation with particular emphasis on freezing rain. Similarly, numerical simulations of accretion have generally addressed the problem of accumulations due to freezing rain (Lozowski and Gayet 1988) or wet snow alone (Kuroiwa 1965; Bauer 1973; Admirat and Sakamoto 1988), although there have been some estimates on the combined effects of these two precipitation types (Finstad et al. 1988).

Little corresponding work has been devoted to understanding the atmospheric production of the physical conditions leading to accretion of precipitation. Almost all of the literature on freezing precipitation[1] is concerned with the development of techniques to predict these situations on the large scale (see for example, Koolwine 1975). Recently however, Stewart (1985) and Stewart and King (1987) have focused on the microphysical aspects of the problem. They predicted that certain combinations of types (snow, ice pellets, and freezing rain) should occur often and that there should be a systematic evolution between these combinations. Stewart and Patenaude (1988) confirmed that such combinations and evolutions do occur.

During the Canadian Atlantic Storms Program (CASP) filed project, detailed measurements were made of precipitation characteristics and accretion near Halifax, Nova Scotia (Stewart et al. 1987). These measurements included a measure of precipitation terminal velocities as well as size spectra and images of the precipitation particles.

This article describes the precipitation and atmospheric characteristics occurring during accretion events and illustrates the detailed understanding of precipitation characteristics that is required before accretion can be accurately simulated.

Corresponding author address: Dr. Ronald E. Stewart, Cloud Physics Research Division, Atmospheric Environment Service, 4905 Dufferin Street, Downsview, Ontario M3H 5T4, Canada.

[1] Freezing precipitation is defined as any precipitation that freezes on contact with a surface at the temperature of the ambient air at or near the Earth's surface (Environment Canada 1978).

2. Accretion observations

To measure accretion, two Rosemount ice detectors—a model 871CB1 and a model 872B11—were collocated at CFB Shearwater in Nova Scotia during the project. The model 871CB1 had been modified to allow icing events to be continuously observed by recording an analog output proportional to the probe tip oscillation frequency (similar to Solak et al. 1988). Except for this, the probe tip geometry (as described by Henderson and Solak 1983) and the operation of the two probes were identical. Both probes were mounted pointing vertically up. The de-icing heater was triggered after accumulations of the equivalent of approximately 0.5 mm uniform water thickness on the probe tip. A YEW 2-pen chart recorder produced a continuous record of the heater-cycle signals of the two probes and the analog signal of the 871CB1.

Accretion events were defined as periods when an icing signal was recorded during precipitation that was also significant enough to trigger the probe heaters. A total of eight accretion events occurred at Shearwater during CASP (Table 1). The trace from the analog probe was used to determine the start and end of the accretion events. Because of the difficulty of relating heater cycles to accretion amounts in variable precipitation, no attempt was made to estimate accretion rates. The total accretion time was 870 min but individual events varied from 45 min to 285 min with an average of 110 min.

Precipitation amounts were recorded every 6 h by the weather observer. Due to the short duration of accretion periods, precipitation rates were estimated from the definitions of precipitation intensity as observed visually by the weather observer (Environment Canada 1978). As indicated in Table 1, average liquid-equivalent precipitation rates during accretion varied from about 1 to about 3 mm h^{-1}.

3. Environmental conditions during accretion

Table 1 indicates the synoptic events that occurred at Shearwater at the approximate times of the accretion events. Accretion was most often associated with a warm front, although on some occasions there was no distinct frontal surface analyzed at the surface.

The surface temperatures experienced during accretion are shown in Fig. 1. The most common temperature was between 0° and −1°C with 65% of the accretion occurring between these values. The coldest temperatures were −4° to −5°C. In contrast, Henderson and Solak (1983) reported that accretion events over the Sierra Nevada Mountains of California were often associated with temperatures colder than −6°C. Minsk (1980) has reported accretion to occur at temperatures down to −20°C, although it was most frequent at temperatures above −3°C.

Accretion almost always occurred during saturated conditions. Over 98% of the accretion occurred in relative humidities above 95%. Fog was reported during 67% of the accretion time. In contrast, blowing snow, which occurs in less humid conditions, was only present for about 25% of the time during accretion.

During accretion events, moderate winds were experienced. Wind speeds were between 5 and 15 m s^{-1} with the average being 7.5 m s^{-1}. The wind direction was typically from the south–east, which is an onshore flow from the Atlantic Ocean. This southeasterly flow was associated with the air motion that typically preceded a warm frontal or trough passage.

4. Precipitation types during accretion

Different precipitation types were associated with accretion (Fig. 2). Single precipitation types, not occurring with other types, occurred during about 73% of the total accretion time. Freezing rain was the most common single precipitation type; snow was the only other significant type that alone was associated with accretion. Combinations of precipitation types occurred for about 27% of the accretion time. Snow with ice pellets was the most common combination, although snow with freezing rain was almost as prevalent.

During some of the accretion events precipitation-type transitions occurred (Fig. 3). Many of the transitions followed an evolution of precipitation types

TABLE 1. Accretion events at Shearwater, Nova Scotia.

Event	Date	Start (UTC)	End (UTC)	Duration (min)	Synoptic situation	Types	Precipitation rate (mm h^{-1})
1	2 Feb	2045	2230	105	warm front	S, SP, ZR, F	1.5
2	5 Feb	1630	1715	45	trough	S, IP, ZR, F	3.0
3	15 Feb	1215	1315	60	trough	S, F	1.5
4	15 Feb	1845	2000	75	trough	S, F	1.5
5	22 Feb	0745	0930	105	warm front	S, IP, ZR, F	3.0
6	7 Mar	1130	1245	75	warm front	S, IP, ZR	2.5
7	11 Mar	0545	1030	285	warm front	S, IP, ZR, F	1.0
8	14 Mar	1730	1930	120	warm front	ZR, F	<1.0

The precipitation types and other terms that are used in this and all other figures are rain (R), freezing rain (ZR), ice pellets (IP), snow pellets (SP), snow (S), and fog (F).

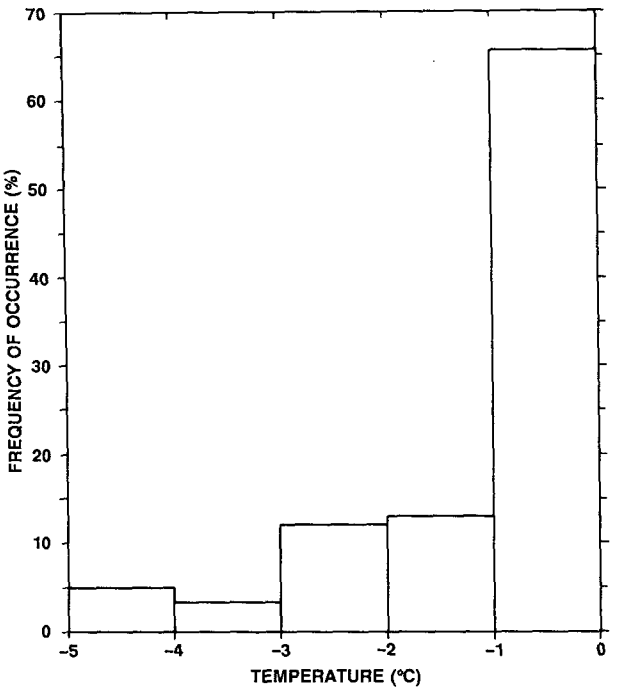

FIG. 1. Frequency of occurrence of surface temperatures during accretion. Temperatures are averages over 15 min periods. There are 58 periods in total.

similar to that predicted by Stewart and King (1987) if there was time for complete refreezing of semimelted particles in the subfreezing region near the surface. The relatively common combination of snow and freezing rain was predicted to occur if complete refreezing had not taken place in the lower atmosphere. This combination implies therefore that at least some of the particles appearing to be drops would actually be composed of both water and ice.

Figure 4 shows the evolution of precipitation types during accretion. Transitions between types occurred at different points during the accretion events. There was also a trend for the longer durations to be predominantly associated with freezing rain alone or with fog.

Five soundings were made from Shearwater during accretion events (Fig. 5). These soundings showed that substantial inversions were present when freezing rain was observed. However, the actual heights of the inversions varied substantially. The base of above-freezing temperatures ranged from 250 m to over 2 km. The one sounding not associated with freezing rain had maximum temperatures that barely exceeded 0°C. Particles in this case would not have melted completely and so no freezing rain was observed at the surface (Stewart 1985).

5. Particle images and spectra during accretion

Particle characteristics during accretion were determined through the use of a ground-based Particle Measuring Systems (PMS) 2DG laser imaging probe, visual observations, and microphotographs. The 2DG probe produces images of particles up to 9.6 mm across with a resolution of 0.15 mm. The 2DG probe collected particle images during six of the cases. Microphotographs of the precipitation particles were obtained from two of the cases.

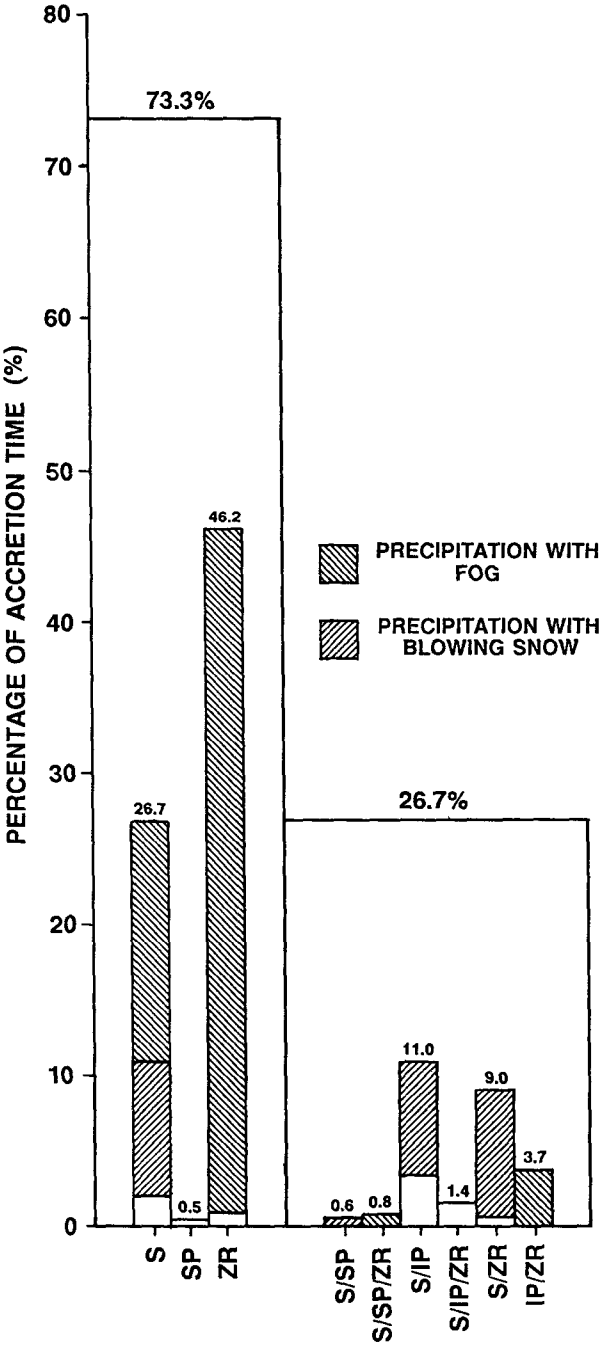

FIG. 2. Fraction of accretion time as a function of precipitation type. The precipitation types are as defined in Table 1.

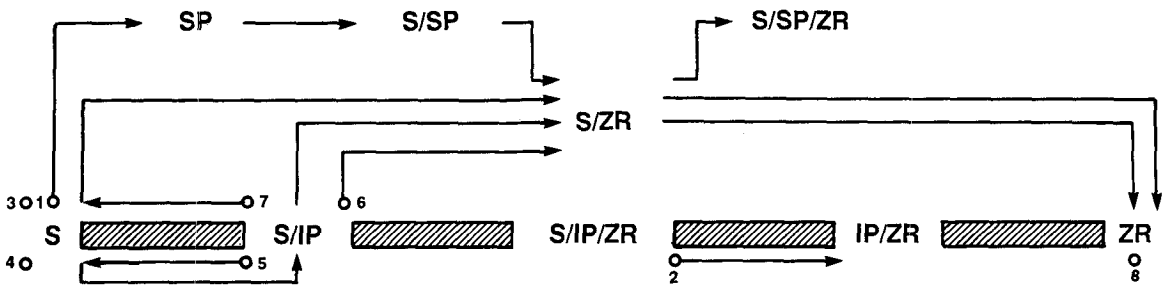

FIG. 3. Precipitation-type evolution during accretion events in comparison with the theoretical predictions of Stewart and King (1987) indicated by the thick bars. The numbers indicate the events shown in Table 1.

To illustrate key features of the precipitation, representative 2DG images from accretion cases are shown in Fig. 6. These images illustrate that the snow was often in the form of aggregates. The largest aggregates were of the order of 9 mm in diameter, although larger ones not detected by the probe due to the probe's maximum sampling width were sometimes reported by the probe operator. Some of the aggregates had rounded edges implying that partial melting and/or riming had occurred. Many of the individual crystals visible in the images were columns and needles. The microphotographs in Fig. 7 show that riming on the particles occurred. Ice pellets were either seen as irregularly shaped particles or as circular particles, which were therefore indistinguishable from liquid drops.

Illustrative particle-size spectra are shown in Fig. 8. Freezing rain with or without ice pellets showed an approximate exponential distribution as described by the work of Marshall and Palmer (1948). However, there was often an excess in the concentration of small drops over that predicted by the Marshal–Palmer distribution. Cases with a combination of all three precipitation types simply showed a wide distribution that was approximately described by an exponential distribution. Similar observations have been made in snow aloft by, for example, Stewart et al. (1984).

6. Particle terminal velocities during accretion

A vertically pointing Doppler radar precipitation occurrence sensor system (POSS) was located at CFB Shearwater. This instrument produced a record of the Doppler velocity spectra of the precipitation and was able to detect Doppler velocities up to 16 m s^{-1}.

The POSS is a low power, continuous wave X-band bistatic system (Sheppard 1989). The transmitter and receiver antenna beams are oriented 20° from the vertical and intersect about 31 cm above the horizontal plane through the antenna radomes. The POSS measures the Doppler velocity spectrum of scatterers in a small volume of air immediately above the sensor. During the measurement sampling interval, a single drop moving at constant velocity produces a varying frequency that depends upon its changing position within the sampling region. Therefore, 100 spectra are averaged every 2 min to produce a volume-averaged Doppler velocity spectrum that has a resolution of about 0.25 m s^{-1} in terminal velocity. The relationship of the Doppler velocity to the terminal velocity is a function of the antenna beam geometry and wind conditions. The velocity associated with the highest returned power, the Doppler mode velocity (DMV), is essentially unaffected by the wind. In contrast, the Doppler spectra is broadened by wind.

Figure 9 shows examples of normalized, Doppler power spectra averaged for 2 min in mixed precipitation. If different precipitation types have different terminal velocities and comparable reflectivities then a multimodal spectra will result with each mode corresponding to an individual type. In spectrum (a) the dominant type was snow with the DMV near 2 m s^{-1}. As indicated by spectra (b) and (c), a DMV value of 4 m s^{-1} often occurred when freezing rain and ice pellets occurred. A secondary peak sometimes also occurred near 5 m s^{-1}. This may be due to freezing rain although insufficient data make this impossible to prove.

To illustrate the evolution of Doppler velocity characteristics, Fig. 10 shows values across the entire accretion event on 22 February. The transition from snow to freezing rain corresponded to an increase in the DMV from about 2 m s^{-1} to 6 m s^{-1}. As expected, a greater range of velocities occurred with freezing rain than with snow. Over the 105 min period of accretion, the Doppler velocities therefore provided substantial insight into the nature of the changing precipitation conditions.

7. Discussion

a. Overview of accretion events

Accretion was associated with a variety of conditions. Accretion usually occurred during moderate winds and temperatures near 0°C. Elsewhere, accretion has been observed at much colder temperatures and higher winds, although this accretion was mostly associated with supercooled droplets rather than with precipitation-sized particles (Solak et al. 1988).

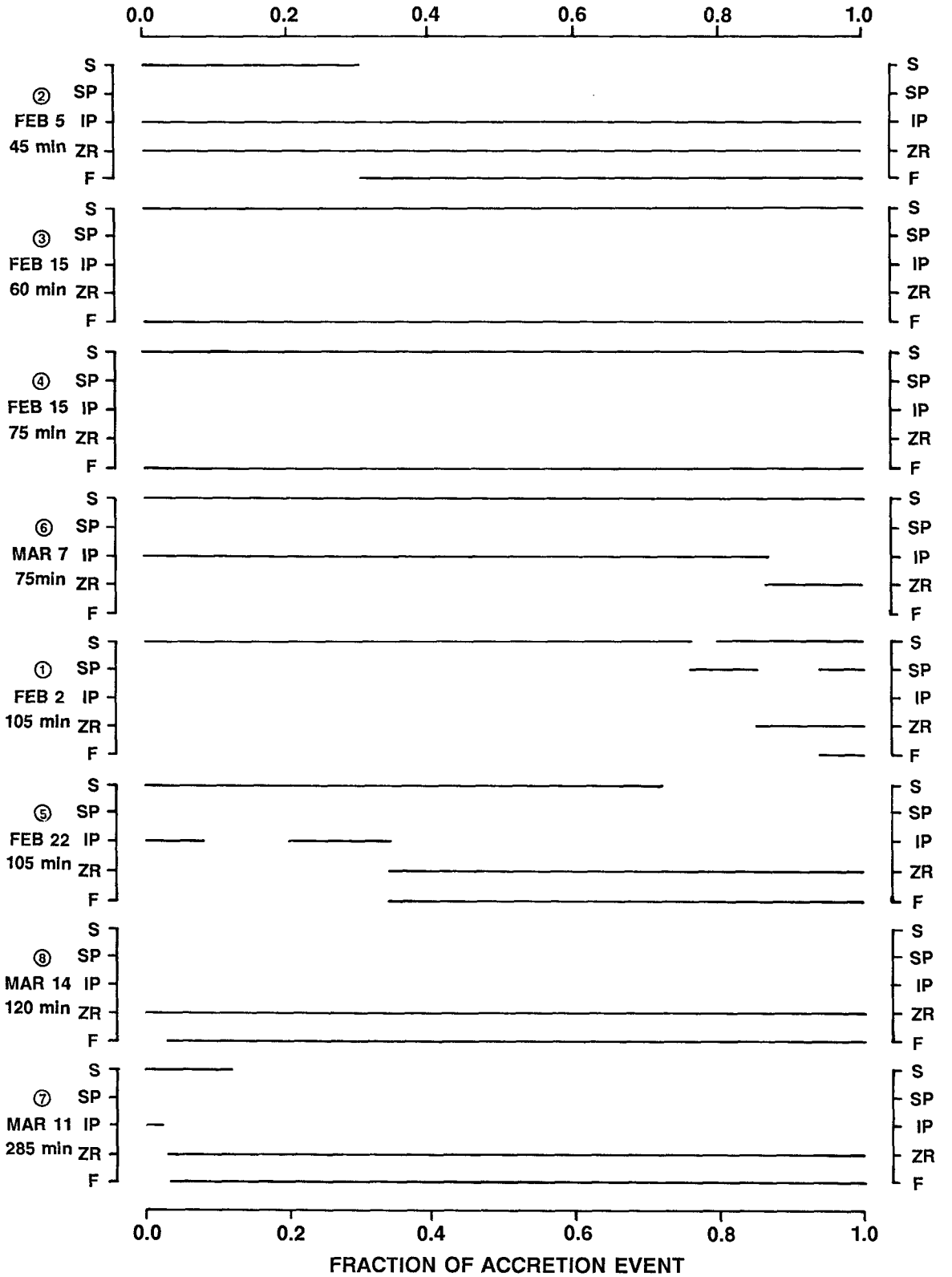

FIG. 4. Normalized precipitation-type transition times for accretion events. The transitions are arranged with total transition time increasing downward.

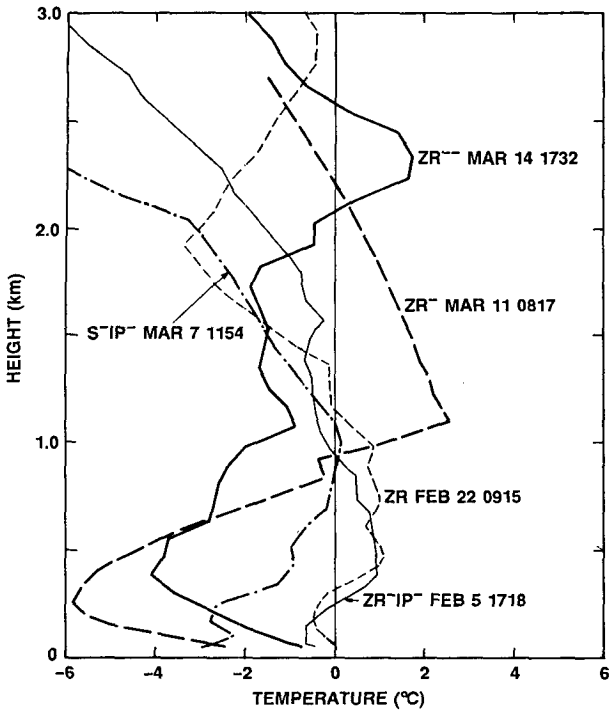

FIG. 5. Vertical profiles of temperature observed at Shearwater during accretion events. The atmosphere was at or near saturation in all cases. Times are UTC.

The observations illustrate that accretion was associated with a number of different precipitation types. Whether a single precipitation type such as snow or freezing rain occurred or whether a complicated pattern of types occurred, substantial accretion resulted. The precipitation-type patterns agreed somewhat with the theoretical predictions of Stewart and King (1987) but departures from the theory often occurred. This is at least partially because the theoretical predictions assumed that the particles had completely refrozen in the lower subfreezing region.

b. *Particle characteristics and impact angles*

The precipitation occurring during accretion was associated with different terminal velocities. Snow was usually associated with the Doppler velocities less than 2.5 m s^{-1}. In freezing rain, the DMV was higher than 2.5 m s^{-1}. Such results are quite consistent with expected values (Appendix). In calm conditions, the particle terminal velocity will affect the nature of its collision with an object. The shape, density, and phase composition of the particle after collision will influence its consequent freezing behavior.

During accretion in windy conditions, the relative magnitudes of the horizontal winds and the terminal velocities will be important. In high winds all particles would move almost horizontally; the difference in terminal velocity would have a negligible effect on the trajectories. In moderate winds in which the horizontal winds and the terminal velocities are of comparable magnitude, particle trajectories will be significantly affected by their terminal velocities, with snow impacting at a more horizontal angle than the faster falling rain. In the present accretion cases, the winds and terminal velocities were of comparable magnitude.

The impact angle is a measure of the deviation of the trajectory from the vertical. In a wind speed of v_h, the impact angle θ of a particle having terminal velocity v_t is given by

$$\theta = \arctan(v_h/v_t). \quad (1)$$

Here, θ is plotted in Fig. 11 as a function of wind speed and terminal velocity. For the typical conditions of winds between 5 and 10 m s^{-1} and for particles falling at less than 10 m s^{-1}, impact angles will always exceed 30°.

The observed terminal velocity results from Fig. 9 have been included in Fig. 11. Minimum impact angles would be about 40° in all cases. The DMV measured by the POSS was associated with impact angles near 67° for the cases on 5 February; this velocity corresponded with angles above 70° in the 2 February case with snow and very light freezing rain. The closeness of the resultant impact angles at the DMV was largely due to the difference in horizontal winds. There would have been an approximate 10° difference in impact angle if the wind speeds had been the same.

It should be noted that turbulence will affect these impact-angle results in some cases. The actual horizontal and vertical motions experienced by the particles would be influenced by the characteristics of the turbulent eddies.

c. *Occurrence of particles composed of liquid and solid*

It is believed that some particles present during accretion were composed of a mixture of water and ice. As mentioned earlier, snow with freezing rain implies that some particles that would appear to be liquid drops were actually composed of a combination of solid and liquid (Stewart and King 1987). Also, some of the images of snow had rounded edges, which implies that some snowflakes had water on them and were therefore wet.

The likelihood that wet snow occurred during some of the accretion events was examined in more detail. Wet snow can form under different conditions. It can 1) be due to melting, 2) occur if sufficient accretion occurs to raise the surface temperature of a snowflake by latent heat release to 0°C, 3) result as snow, partially melted aloft, is refreezing within subfreezing conditions near the surface, or 4) result from the collisions of snowflakes with freezing rain drops.

All of the accretion events occurred at subfreezing surface temperatures. The first possibility that the snow

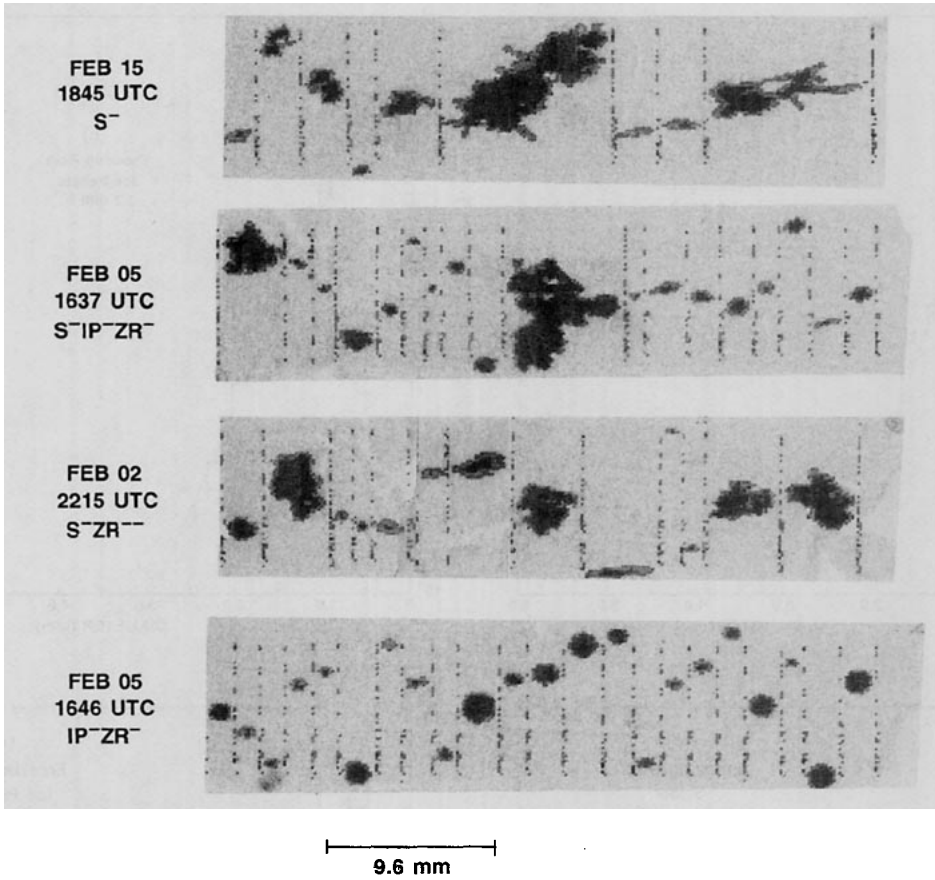

FIG. 6. Images of particles from the 2D ground probe during accretion. The precipitation types are also shown.

was wet during melting, therefore, did not apply to these accretion studies.

Many of the snowflakes were subjected to some riming. The surface temperatures of the snowflakes during accretion can be determined by a balance between the heating due to riming and condensation, and cooling due to sensible heat loss. Assuming that the snowflakes are spheres and that conditions are at steady state, the heat balance of the snowflake is given by

$$L_f \frac{dm}{dt} = -2\pi D_s k_a F_h (T - T_s) - 2\pi D_s L_e F_v D_v (e - e_s). \quad (2)$$

Here, dm/dt is the rate at which water is riming onto the particle, D_s is the snowflake diameter, T is the air temperature in °C, T_s is the snowflake surface temperature assumed to be 0°C, e is the vapor pressure in the air, and e_s is the vapor pressure at the snowflake surface. Here, L_e and L_f are the latent heats of evaporation and fusion respectively, k_a is the thermal conductivity of air, D_v is the diffusivity of water vapor in air. Here, F_h and F_v are the mean ventilation coefficients for heat and water vapor fluxes respectively (Pruppacher and Klett 1978).

Calculations with moderate riming rates indicate that a snowflake's temperature should rise about 0.3°–0.5°C above its value in the absence of riming. For the cases in which snow alone was associated with accretion, 1215–1315 UTC and 1845–2000 UTC 5 February

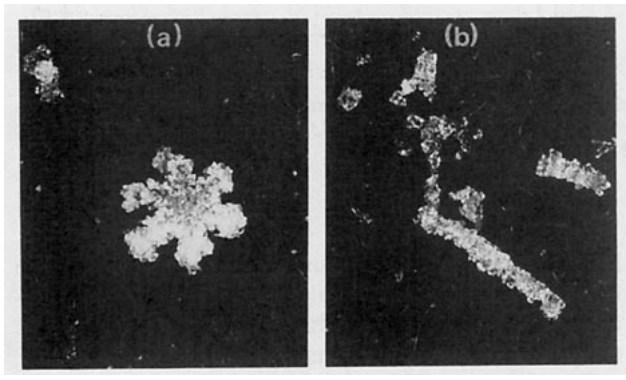

FIG. 7. Photographs of ice crystals sampled at (a) 2048 UTC, and (b) 2050 UTC 2 February 1986. The height of each photograph corresponds to 9 mm.

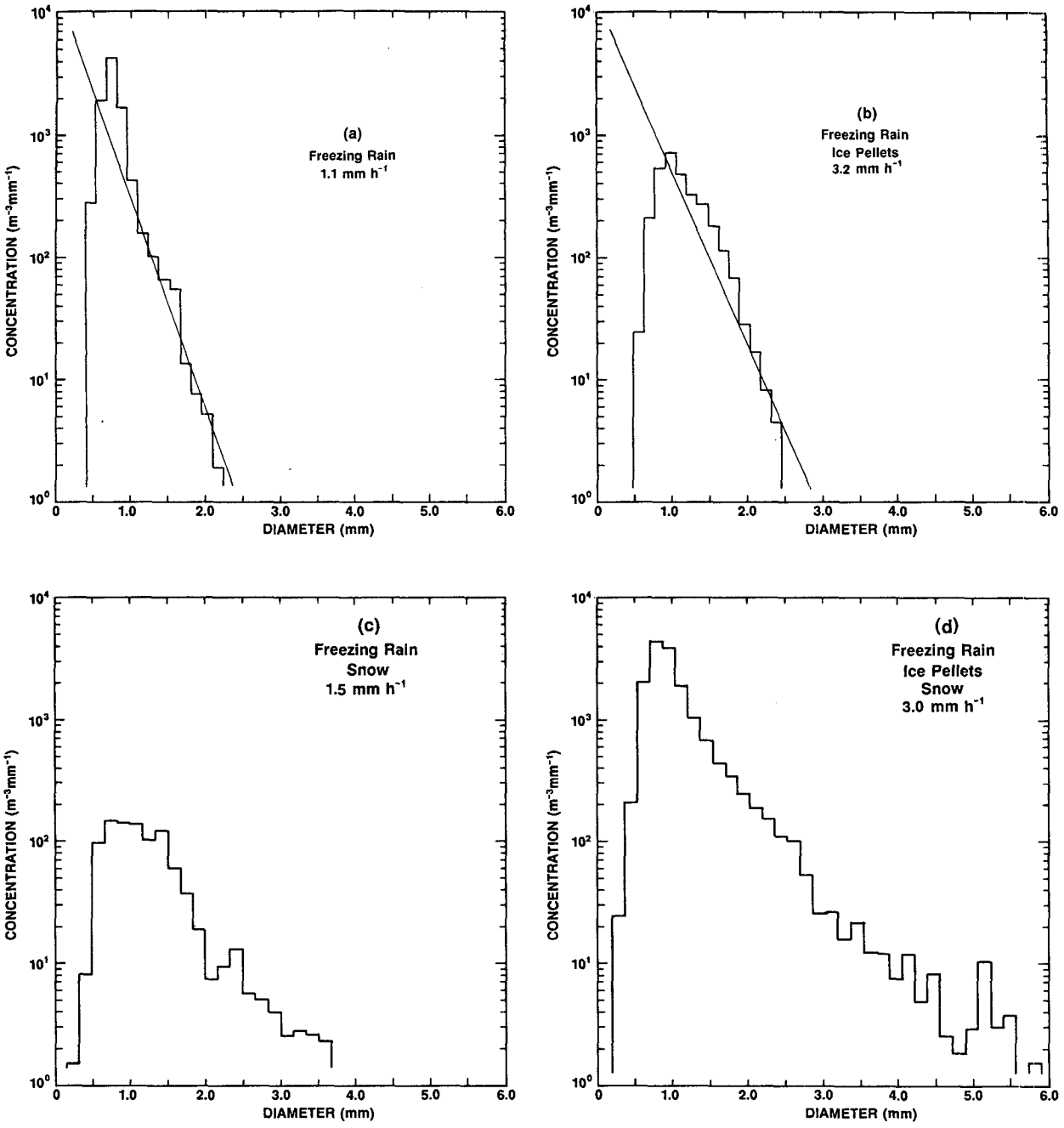

FIG. 8. Particle-size spectra during accretion. The Marshall–Palmer distributions are indicated in (a) and (b) and the precipitation types and precipitation rates are also shown. The times at which the spectra were obtained are (a) 0640–0700 UTC on 11 March, (b) 1643–1649 UTC on 5 February, (c) 2214–2300 UTC on 2 February and (d) 1630–1643 UTC on 5 February 1986.

for example, surface temperatures were always within a degree of 0°C. One would expect that the bulk temperature of some of the snowflakes could therefore reach 0°C in these cases. Local temperatures on the surface of the snowflake where accretion is actually occurring may be higher than predicted by the bulk approach. When this is considered as well, the likelihood that liquid existed on some snowflakes is even higher. In general, these calculations are quite consistent with the observations that some accretion occurred only during snow situations.

The third possibility for producing wet snow due to incomplete refreezing within the subfreezing region is supported by the common occurrence of ice pellets or

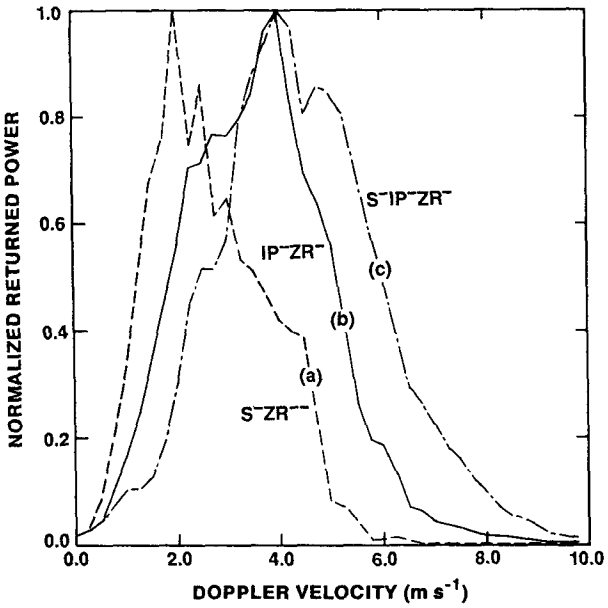

FIG. 9. The normalized Doppler velocity spectra measured by the POSS for three periods of accretion. The precipitation types occurring at these times are shown on the figure. The spectra are 2 min averages: (a) occurred from 2221–2223 UTC on 2 February, (b) occurred from 1648–1650 UTC on 5 February, and (c) occurred from 1635–1637 UTC on 5 February. The minus sign (−) indicates that the precipitation intensity was light, and (−−) indicates a very light intensity.

freezing rain with the snow. The possibility of partial freezing below an inversion was examined further. If condensation, evaporation, and sublimation are not considered, the rate at which a snowflake refreezes is given by:

$$L_f \frac{dM}{dt} = -2\pi D_s k_a F_h (T - T_s). \tag{3}$$

Here, dM/dt is the rate of freezing of a snowflake. For snow, Matsuo and Sasyo (1981) have formulated the Nusselt number, Nu, as

$$\mathrm{Nu} = 2F_h = 3.5(1 + 0.275\ \mathrm{Pr}^{0.33}[v_t D_s \rho_a/\mu]^{1/2}). \tag{4}$$

Here, Pr is the Prandtl number of order unity. The term within the square brackets is the Reynolds number, ρ_a is the air density, and μ is the dynamic viscosity. For particles larger than approximately 1 cm in diameter, the second term within the parentheses is substantially greater than 1.

Assuming that the air temperature is constant and the snow particle maintains a spherical shape and falls at a constant terminal velocity during refreezing, the time required for complete refreezing can be estimated. This time is given simply by the mass that needs to be

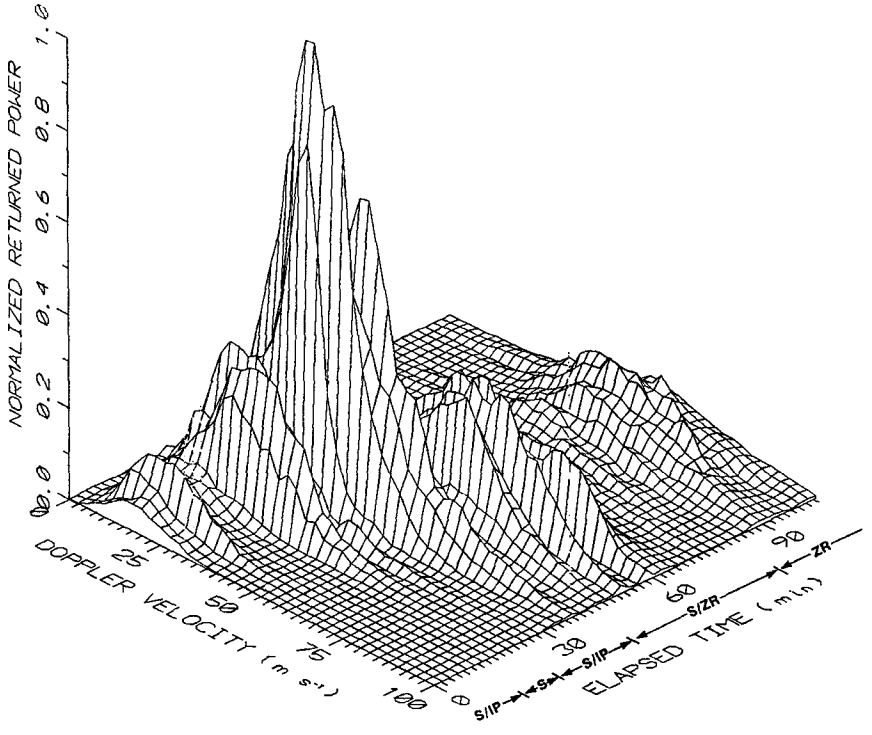

FIG. 10. The normalized Doppler velocity spectra measured by the POSS as a function of elapsed time and precipitation type on 22 February 1986. The starting time was 0745 UTC. The power is normalized with respect to the maximum returned power during the period.

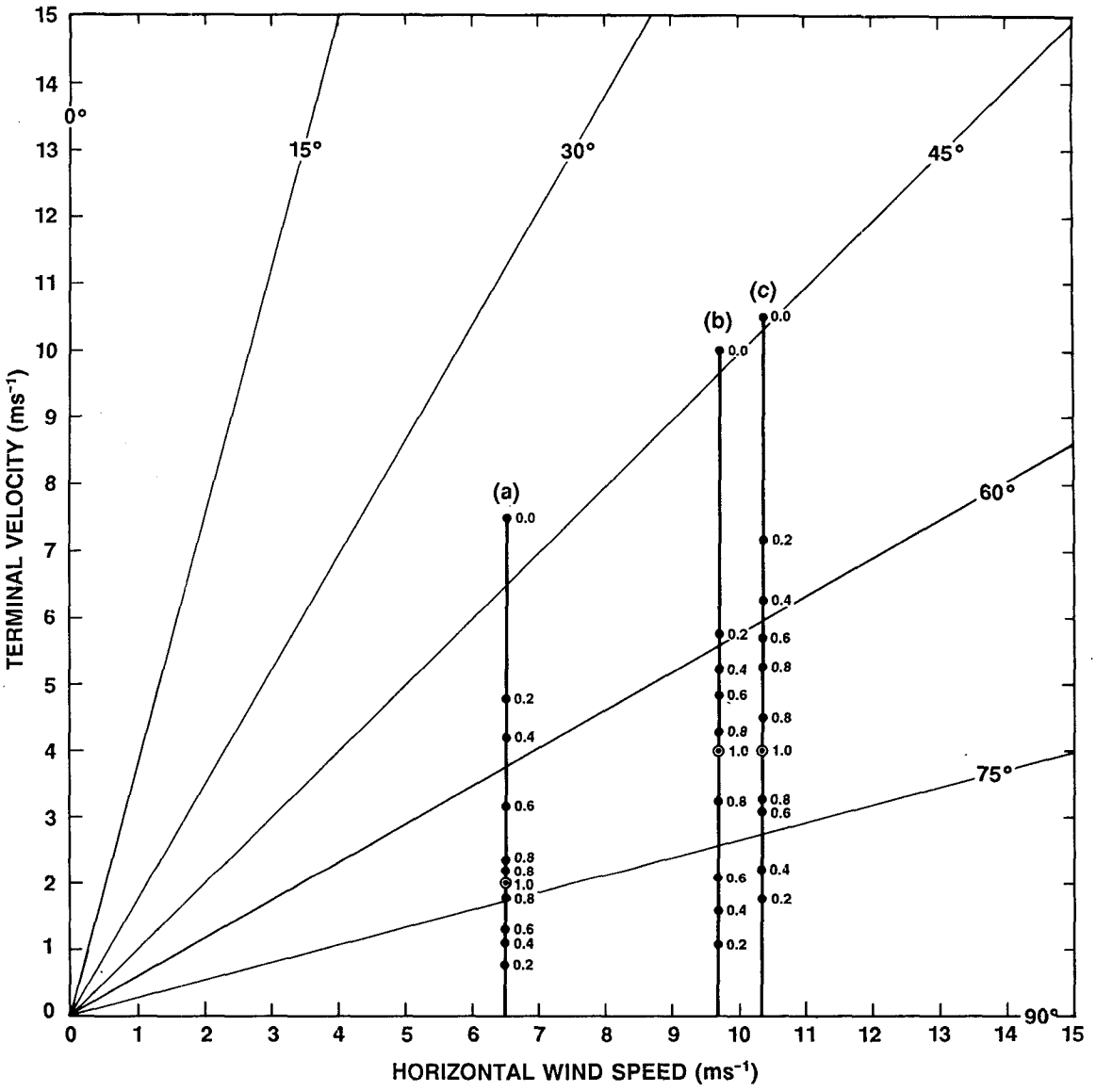

FIG. 11. Impact angle as a function of terminal velocity and wind speed. The three lines refer to the POSS normalized, returned power information from Fig. 9 and the numbers on these lines refer to values of normalized power. The lines have been superimposed onto this diagram at the wind speeds occurring at the appropriate times. As in Fig. 9, the lines refer to (a) 2 February at 2221–2223 UTC, (b) 5 February at 1648–1650 UTC, and (c) 5 February at 1635–1637 UTC.

refrozen divided by the rate at which it is being frozen. The time to completely refreeze, t_f, is given by

$$t_f = -L_f \rho_s D_s^2 / [12 k_a F_h (T - T_s)]. \quad (5)$$

Here ρ_s is the density of the snowflake. The time available for refreezing t_a is simply given by the length of time that the particle spends within the subfreezing conditions that exist over a depth H. The time is given by

$$t_a = H / v_t. \quad (6)$$

The fraction, f_s, of the snowflake that is liquid at the surface can then be expressed in terms of these times. Here, f_s, which must range between 0 and 1, is given by

$$f_s = f_o + 5.8 \left(\frac{H k_a T}{L_f \rho_s} \right) \left(\frac{\rho_a}{v_t D_s^3 \mu} \right)^{1/2} \quad (7)$$

where f_o is the fraction of the snowflake that was initially liquid, and T_s of 0°C has been utilized.

The depth of the subfreezing layer and the average atmospheric temperatures leading to complete refreez-

ing based on Eq. (7) are plotted in Fig. 12. It was assumed that a snowflake initially contained a substantial amount of water but the snowflake had not collapsed (see for example, Matsuo and Sasyo 1981; Knight 1979). Furthermore, its terminal velocity was set at 1.75 m s^{-1} to reflect a lower drag coefficient than if no water was present. The conditions required for complete refreezing vary substantially with particle size and initial fraction. This furthermore indicates the extreme sensitivity of the wet snow calculations to conditions occurring aloft which control the initial amount of melting.

As shown in Fig. 5, a sounding was made on 7 March during an accretion event in which snow was occurring. The depth of the subfreezing region as well as its average temperature have been superimposed onto Fig. 12. In this instance, the calculations indicate that only snowflakes larger than about 2 cm would have reached the surface without refreezing. Smaller snowflakes could have reached the surface unfrozen if they had a terminal velocity or density higher than the values used in the calculations. In contrast, if snowflakes had occurred on 5 or 22 February, snowflakes smaller than 1 cm would not have frozen even if they were only 30% water initially.

The last means of producing wet snow is by the collision of a snowflake with a liquid drop within the subfreezing region above the surface. If it does not break up, the resultant particle will be composed of a mixture of liquid and solid, although, it would of course start to freeze according to the preceding discussion. The likelihood that a snowflake will collide with a drop can be estimated by considering the number of drops that will collide with a snowflake as the snowflake falls through the subfreezing region. Assuming that the collection efficiency is unity and the snowflake is substantially larger than the drops, the number of collisions N is given by

$$N = n\pi D_s^2(v_d - v_t)t_a/4. \quad (8)$$

Here, n is the concentration of drops, v_d is the drop terminal velocity, and the time in the subfreezing region is given by Eq. (6). In this situation, the drops are overtaking the snowflake.

The probability of a collision can be estimated. Assume the number concentration of drops is about 10 m^{-3}, the diameter of the snowflake is 1 cm, the terminal velocity of the drops is 5 m s^{-1}, and the terminal velocity of the snowflake is 1 m s^{-1}. Equation (8) then predicts that a collision will occur of the order of once every 100 m. This process may be quite important in leading to wet snow in situations when a combination of precipitation types are occurring. This process will furthermore act to reduce the number of particles which accrete as pure liquid in such situations.

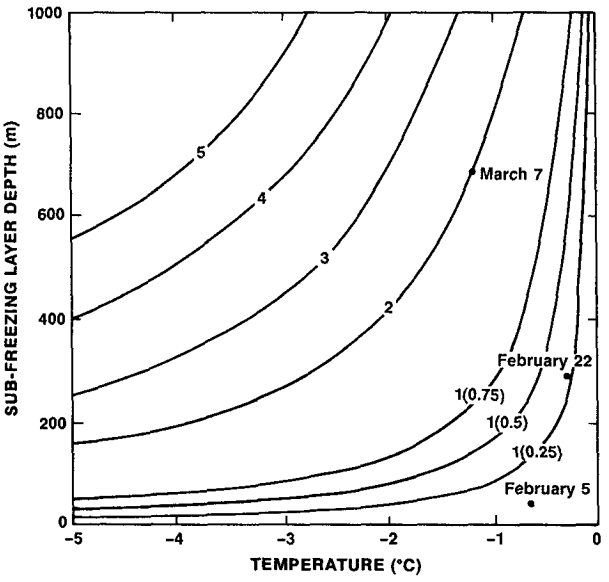

FIG. 12. The depth of the subfreezing layer and average atmospheric temperatures leading to the complete refreezing of snowflakes. The diameter (cm) of snowflakes is indicated. It is assumed that the initial liquid fraction of the solid lines for diameters above 1 cm is 0.75. For a 1 cm diameter, the number in brackets indicates the value of the initial liquid fraction. It is further assumed that the terminal velocity is 1.75 m s^{-1} and the snowflake density is 25 kg m^{-3}. Observed depths and temperatures from three cases plotted in Fig. 5 have been included as well.

d. Accretion by particles composed of liquid and solid

It is believed that some particles during accretion were composed of a mixture of liquid and solid. A model was used to examine some of the effects of such particles on accretion.

In the current model the icing rate at the stagnation point of a 2.54 cm diameter cylinder was calculated using a quasisteady state heat-balance approach similar to Lozowski et al. (1983). While acknowledging the complexities involved in freezing an ice/water mixture within the impacting drops, a simple first approximation is that the latent heat released during accretion is reduced due to the pre-existing ice portion of the particles. This may be simply modeled by reducing the latent heat of fusion, L_f, without changing the other particle properties. The reduced latent heat release is then given by $f_s L_f$ where f_s is the fraction of the particle that is liquid.

Illustrative accretion results are shown in Fig. 13. In these calculations a liquid drop of 1 mm diameter was considered. For the conditions examined, there was little change in the normalized accretion rate when temperatures were colder than −1°C. Freezing occurred so quickly for both wind speeds that the difference in latent heat release was insignificant. For temperatures warmer than −1°C there was a dramatic in-

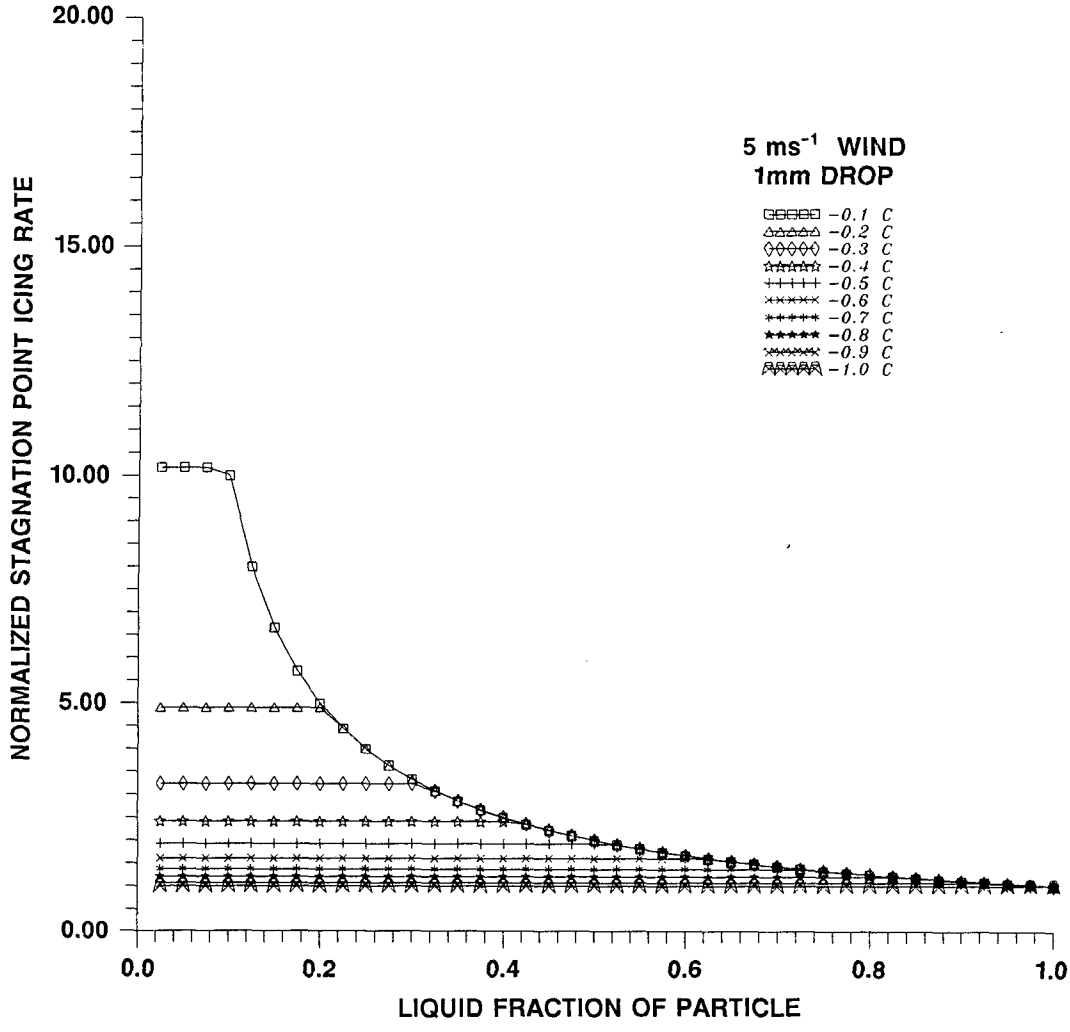

FIG. 13. Normalized accretion rate on a 2.54-cm diameter cylinder as a function of temperature, wind speed [(a) 5 m s^{-1}, (b) 10 m s^{-1}], and the liquid fraction of the particle. The normalized rates were computed from the predicted accretion rate of a particle relative to the rate for a pure liquid particle.

crease in the normalized accretion rate as the fraction of liquid was decreased. The difference in latent heat released allowed freezing to occur at a substantially faster rate than in the pure liquid situation. The impacted liquid would not, therefore, be able to move as far away from the stagnation point before freezing had been completed and the accretion rate at the stagnation point would be correspondingly higher. For each temperature, there was also a critical fraction of liquid below which there was no difference in the normalized accretion rate. This critical temperature must be associated with the conditions needed for rapid freezing in place; lower fractions of liquid would only cause faster freezing, but at the stagnation point. Increasing the wind speed was associated with a substantial increase in the influence of the liquid fraction. Because freezing occurs faster for particles composed of a mixture of liquid and ice, an impacted particle that was initially a mixture of phases is not swept as far away from the stagnation point before freezing as would be an initially liquid particle. This effect, resulting in an increase of normalized accretion rate, would be enhanced with increasing wind speed.

These model results, therefore, illustrate the sensitivity of accretion to the nature of the particles as well as to other environmental conditions. As previously noted, 65% of the accretion occurred at temperatures between $-1°$ and 0°C; this is just the range over which the effect of liquid fraction is significant. Furthermore, the observed winds with typical values of 5–10 m s^{-1} are strong enough to accentuate the effects of the particle nature.

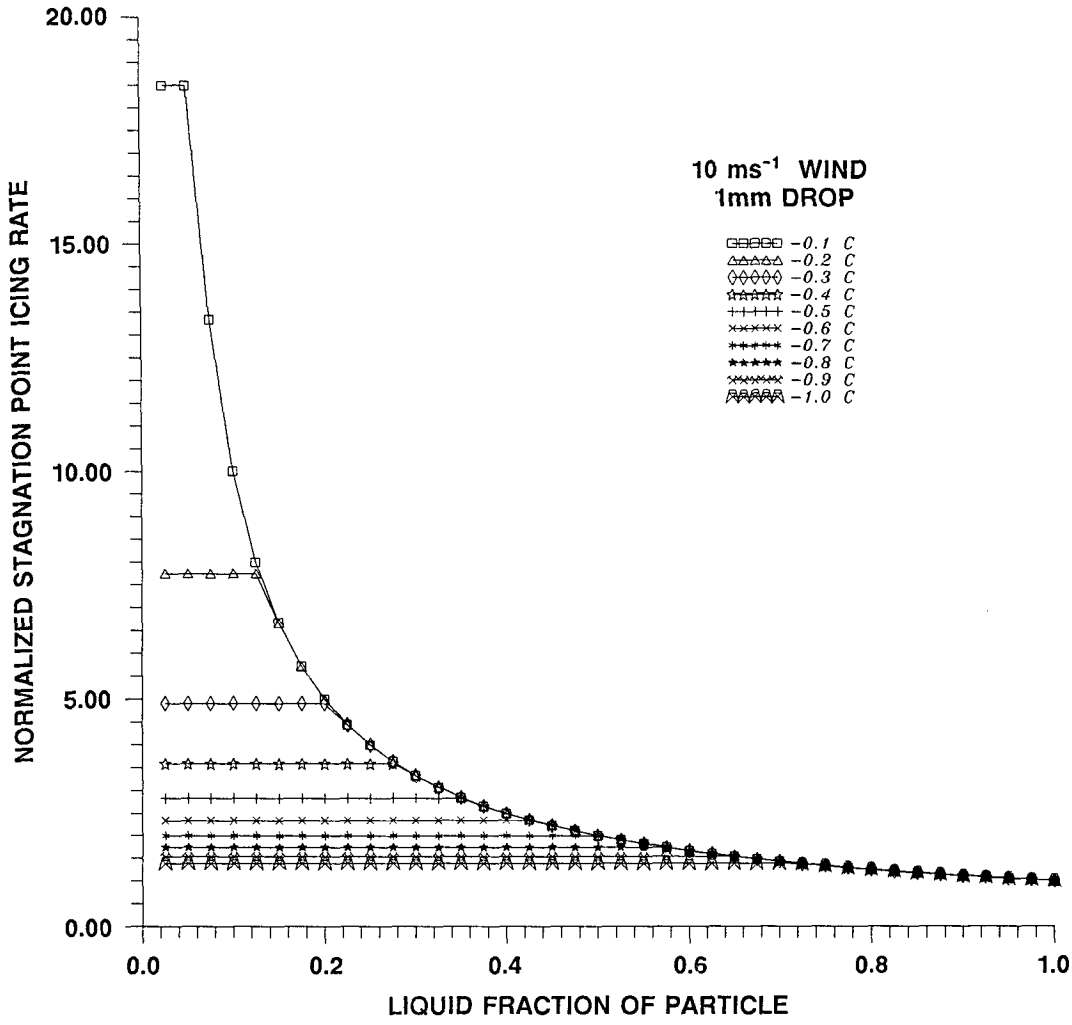

FIG. 13. (*Continued*)

8. Concluding remarks

Accretion in Canadian east coast storms occurs within different precipitation-type and environmental conditions. The actual accretion on structures is a complicated outcome of the detailed precipitation-type characteristics, environmental conditions, as well as structural conditions.

An accurate measurement of all the above factors, especially the nature of the precipitation, is needed before proper accretion modeling can be conducted. Critical characteristics of the precipitation include sizes and densities, phases within the particles, and terminal velocities. The occurrence of liquid within particles such as wet snow could not be directly determined by the available instruments in this study, even though it is a critical parameter in many of the accretion cases.

In summary, this study has pointed out the complexities of the precipitation associated with accretion. Better prediction of accretion events must properly incorporate the detailed nature of the precipitation.

Acknowledgments. This research was supported by the Federal panel on Energy Research and Development (PERD). The authors would also like to thank R. Wilson and the late M. Woodhead for their documentation of the accretion probe information.

APPENDIX

Particle Terminal Velocities in Different Conditions

The rate of accretion of particles is greatly dependent on their velocity. The horizontal motion of precipitation particles is normally very close to that of the mean wind speed, but it can vary due to turbulence near the ground. The vertical velocity is more difficult to predict. It is a combination of vertical air motion and the particle's terminal velocity. The terminal velocity is a bal-

ance between gravity and the drag force, and it therefore depends upon the particle's shape, size and density, as well as the air density. A brief discussion of terminal velocity follows but more extensive examinations can be found in, for example, Rogers (1979) or Pruppacher and Klett (1978).

The terminal velocity of rain is a well-defined function of size since density is constant and shape depends only on size (Gunn and Kinzer 1949). The terminal velocity increases as the square root of the radius to a rough first-order, for precipitation sizes, but more accurate formulations incorporating variations in Reynolds number and shape are available (see for example, Beard 1976). Terminal velocities vary from 0.3 m s^{-1} for diameters of 0.1 mm to 9 m s^{-1} for diameters of 6 mm.

For snow crystals and aggregates the prediction of terminal velocity is more complicated (Langleben 1954). The shapes and densities vary radically from one particle type to another, and the terminal velocity of an individual particle may even vary if it is tumbling. Locatelli and Hobbs (1974) give examples of empirical fits to observed fall velocities of various solid particles. For aggregates (snowflakes) the maximum velocity is in the vicinity of 1.5 m s^{-1}, although terminal velocities of large snowflakes up to 2.5 m s^{-1} have been reported for large (>3 cm diameter) snowflakes by Auer (1971). Furthermore, accretion on the snowflakes would be expected to increase terminal velocities. Graupel terminal velocities in excess of 3 m s^{-1} have been reported.

No work has been conducted on the terminal velocities of semimelted particles. It is probable that they will behave like solid particles of intermediate density until they have almost entirely melted, so that their internal crystal structure breaks down (Matsuo and Sasyo 1981). These particles will have terminal velocities between particles of solid and liquid precipitation of the same mass.

REFERENCES

Admirat, P., and Y. Sakamoto, 1988: Wet snow on overhead lines: State-of-art. *Proc. Fourth Conf. Atmos. Icing Structures,* Paris, 7–13.

Auer, A. H., 1971: Some large snowflakes. *Weather,* **26,** 121–122.

Bauer, D., 1973: Snow accretion on power lines. *Atmosphere,* **11,** 88–96.

Beard, K. V., 1976: Terminal velocity and shape of cloud and precipitation drops aloft. *J. Atmos. Sci.,* **33,** 851–864.

Environment Canada, 1978: Manual of climatological observations. Downsview, Ontario, 61–64.

Finstad, K. J., S. M. Fikke and M. Ervik, 1988: A comprehensive deterministic model for transmission line icing applied to laboratory and field observations. *Proc. Fourth Conf. Atmos. Icing Structures,* Paris, 227–231.

Gunn, R., and G. D. Kinzer, 1949: The terminal velocity of fall for water droplets in stagnant air. *J. Meteor.,* **6,** 243–248.

Henderson, T. J., and M. E. Solak, 1983: Supercooled liquid water concentrations in winter orographic clouds from ground-based ice accretion measurements. *J. Wea. Mod.,* **15,** 64–70.

Knight, C. A., 1979: Observations of the morphology of melting snow. *J. Atmos. Sci.,* **36,** 1123–1130.

Koolwine, T., 1975: Freezing rain. M.S. thesis, University of Toronto, 92 pp.

Kuroiwa, D., 1965: Icing and snow accretion on electrical wires. USA Cold Regions Research and Engineering Laboratory, CRREL Res. Rep. 123, 14 pp.

Langleben, M. P., 1954: The terminal velocity of snowflakes. *Quart. J. Roy. Meteor. Soc.,* **80,** 174–181.

Locatelli, J. D., and P. V. Hobbs, 1974: Fall speeds and masses of solid precipitation particles. *J. Geophys. Res.,* **79,** 2185–2198.

Lozowski, E. P., and J. P. Gayet, 1988: The atmospheric icing: A review. *Proc. Fourth Conf. Atmos. Icing Structures,* Paris, 1–6.

——, J. R. Stallabrass and P. F. Hearty, 1983: The icing of an unheated nonrotating cylinder. Part I: A simulation model, *J. Climate Appl. Meteor.,* **22,** 2053–2062.

Makkonen, L., 1984: Modelling ice accretion on wires. *J. Climate Appl. Meteor.,* **23,** 929–939.

Marshall, J. S., and N. Palmer, 1948: The distribution of raindrops with size. *J. Meteor.,* **5,** 165–166.

Matsuo, T., and Y. Sasyo, 1981: Melting of snowflakes below freezing level in the atmosphere. *J. Meteorol. Soc. Jpn.,* **59,** 10–24.

Minsk, L. D., 1980: Icing on structures. USA Cold Regions Research and Engineering Laboratory. CRREL Rep. 80–31, 22 pp.

Pruppacher, H. R., and J. D. Klett, 1978: *Microphysics of Clouds and Precipitation.* D. Reidel, 714 pp.

Rogers, R. R., 1979: *A Short Course in Cloud Physics.* Pergamon, 232 pp.

Sheppard, B. E., 1989: The measurement of raindrop size distributions using a small Doppler radar. *J. Atmos. Oceanic Technol.,* in press.

Solak, M. E., R. B. Allan and T. J. Henderson, 1988: Ground-based supercooled liquid water measurements in winter orographic clouds. *J. Wea. Mod.,* **20,** 9–18.

Stewart, R. E., 1985: Precipitation types in winter storms. *PAGEOPH,* **123,** 597–609.

——, and P. King, 1987: Freezing precipitation in winter storms. *Mon. Wea. Rev.,* **115,** 1270–1279.

——, and L. M. Patenaude, 1988: Rain–snow boundaries and freezing precipitation in Canadian East Coast winter storms. *Atmos. Ocean,* **26,** 377–398.

——, J. D. Marwitz, J. C. Pace and R. E. Carbone, 1984: Characteristics through the melting layer of stratiform clouds. *J. Atmos. Sci.,* **41,** 3227–3237.

——, R. W. Shaw and G. A. Isaac, 1987: Canadian Atlantic Storms Program: The meteorological field project. *Bull. Amer. Meteor. Soc.,* **68,** 338–345.